Blast Resistance of Steel Plate Shear Walls Designed for Seismic Loading

Gordon P. Warn, M.ASCE[1]; and Michel Bruneau, F.ASCE[2]

Abstract: Steel plate shear walls (SPSWs) have become an increasingly popular lateral force resisting system in buildings. Although originally conceived to resist earthquake forces, recent developments raised questions as to the ability of SPSWs to resist blast loading, whereby the plate would resist out-of-plane impulsive pressures. To investigate this, two 0.4-scale single story SPSW specimens, representing the first story of a four story prototype SPSW, were fabricated and subjected to explosive charges. The out-of-plane resistance of the infill plate was analyzed using nonlinear finite-element analysis (FEA) and yield line theory. Results of these analyses showed the out-of-plane resistance is governed by the large deformations and inelastic material behavior and that yield line theory significantly underestimated the out-of-plane resistance in comparison with the finite-element analysis for infill plates typical of SPSW construction. Based on these results a simplified plastic analysis procedure is proposed to estimate the out-of-plane resistance of SPSW infill plates that is shown to agree well with the results of the FEA. Results of the experimental investigation showed the SPSW had a limited capacity to resist out-of-plane blast loading and that the typical seismic detail for connecting the infill plate to the boundary frame might not be appropriate for blast applications.

DOI: 10.1061/(ASCE)ST.1943-541X.0000055

CE Database subject headings: Steel plates; Shear walls; Blast loads; Experimentation; Seismic effects.

Introduction

Steel plate shear walls (SPSWs) have been used as a lateral force resisting system in buildings to provide wind or seismic resistance (Driver and Grondin 2001; Romero 2003; Seilie and Hooper 2005; Sabelli and Bruneau 2006). Typical SPSW framing systems consist of a thin unstiffened infill plate connected to a boundary frame through fishplates (Driver et al. 1997; Schumacher et al. 1999). Under these lateral loading forces applied in the plane of the SPSW, the infill plate buckles in shear, developing diagonal tension field action that resists lateral forces (Timler and Kulak 1983; Driver et al. 1997; Berman and Bruneau 2003). Yet, little is known regarding their resistance to blast—a hazard that is receiving considerable attention in light of an increased awareness in recent years to the risk of intentional or unintended explosions.

Building facades and exterior walls can be designed or reinforced (Norville and Conrath 2006; Simmons et al. 2008) to prevent fragmentation of the exterior façade and the associated debris from penetrating the building envelope in the event of an explosion. When designed for blast loading or reinforced, it is understood that the cladding system (often considered a nonstructural system) will interact with the primary structure capturing much of the blast pressures and distributing the load (or a portion of the load) to the primary structural system (Starr and Krauthammer 2005). Similarly, one could envision the infills of SPSWs to have some inherent blast resistance where the solid surface of the infill catches the entire blast pressure wave (just like other exposed wall or cladding systems) preventing blast waves and associated debris from penetrating a particular area of the building. Design for satisfactory blast performance can be envisioned if procedures and details can be developed to take advantage of the inherent ductility of steel when the SPSW deforms out-of-plane as a membrane. In that perspective, some designs have already been proposed, such as an innovative air traffic control tower concept relying on SPSW to resist both blast and earthquake forces [see Rogers (2002) for the prototype developed for the Federal Aviation Administration (FAA)]. Other contemplated applications include blast-resistant walls needed in confined spaces, such as secure mailrooms and indoor truck delivery bays (John Hooper, Structural Engineer, Magnusson Klemencic Associates, personal communication 2009). One potential benefit that SPSWs as blast resistant walls offer over alternative reinforced curtain wall systems is that the load applied by the SPSW infill plate to the surround structural framing would be limited by the yield strength (assuming the strain level is sufficiently small to avoid strain hardening) and the deformed geometry of the SPSW infill plate. Although the merits of using SPSWs for blast resistant design can be (and have been) advocated based primarily on the results of nonlinear dynamic finite-element (FE) analyses that show promising performance in resisting substantial out-of-plane impulsive loading and sustaining large inelastic deformations, there has been no experimental validation of such a concept.

The objective of the testing program presented in this paper was to investigate the performance of an SPSW designed for seismic loading (with no special considerations for blast) subjected to a reasonably sized explosive threat (i.e., vehicle). To accomplish this, two 0.4-scale SPSW were designed and fabricated based on a prototype SPSW designed for seismic loading. Prior to experi-

[1]Assistant Professor, Dept. of Civil and Environmental Engineering, Penn State Univ., University Park, PA 16802 (corresponding author). E-mail: gwarn@engr.psu.edu

[2]Professor, Dept. of CSEE, Univ. at Buffalo, Amherst, NY 14260. E-mail: bruneau@buffalo.edu

Note. This manuscript was submitted on August 15, 2008; approved on March 30, 2009; published online on May 2, 2009. Discussion period open until March 1, 2010; separate discussions must be submitted for individual papers. This paper is part of the ***Journal of Structural Engineering***, Vol. 135, No. 10, October 1, 2009. ©ASCE, ISSN 0733-9445/2009/10-1222–1230/$25.00.

mental testing of the two model SPSWs, analyses were conducted to predict the out-of-plane resistance of the thin infill plate and to estimate the response of the plate under blast loading. Based on the results of these analyses, an approximate plastic analysis procedure is proposed for estimating the out-of-plane resistance of SPSW infill plates.

While full-scale testing has sometimes been perceived as being preferable to scale testing, scale testing has been extensively used in the past and proven to provide reliable results in all subdisciplines of structural engineering. It has also gained substantial acceptance in blast engineering over the past decade. In particular, blast tests to collapse of quarter-scale reinforced concrete frames (Woodson and Baylot 1999) provided key knowledge on understanding the behavior of concrete buildings, and recent tests did the same for bridges [Williams et al. (2008); Dr. James Ray, U.S. Army Corps of Engineers, personal communication, 2008; and Fujikura et al. (2008), to name a few]. Furthermore, scale testing also provides due consideration of economic constraints (whereas cost of the specimen and reaction frame vary with the scale factor times exponent three) and limitations of the size of the charge that could be detonated at the facility where testing is conducted—a general benefit that was also particularly relevant for the research reported herein.

Prototype Structure and SPSW

The MCEER Demonstration Hospital (Yang and Whittaker 2002; Wanitkorkul and Filiatrault 2008) was chosen as the basis for the design of the prototype SPSW. The MCEER Demonstration Hospital is a four-story steel framed building with 4 lateral-load resisting frames in the north-south direction. To facilitate the design of the prototype SPSW, the structure was assumed to have one 4.9-m wide multistory SPSW in the exterior bay of each of the four lateral force resisting frames. Story heights were 3.8 m, except for the first story at 4.1 m. For the calculation of the earthquake loading the structure was assumed to be located on a stiff-soil site, Site Class D (FEMA 2003). The SPSW was then designed in accordance with ASCE 7–05 (ASCE 2005), the AISC Seismic Provisions (AISC 2005a) and the equivalent lateral force procedure (FEMA 2003)—using a response modification factor, R, of 8 and an importance factor, I, of 1.5 corresponding to Seismic Use Group III (FEMA 2003). The infill (web) plate thickness, t_w, of a particular story was then calculated to resist the entire story shear acting on the frame, according to

$$V_n = 0.42F_y t_w L_{cf} \sin 2\alpha \quad (1)$$

where F_y=yield strength of the infill plate; L_{cf}=clear distance between vertical boundary frame elements (VBE) flanges; α=angle of web yielding (tension field angle); and V_n=nominal strength of the SPSW. For the design of the prototype SPSW the infill plate and boundary frame elements were assumed to be ASTM A572 Grade 50 with a minimum specified yield strength, F_y, of 348 MPa (50 ksi). Table 1 presents a summary of the required infill plate thickness, calculated using Eq. (1) and the specified thickness of 4.8 mm (0.1875 in) for all stories based on the minimum available plate thickness for ASTM A572 Grade 50.

The boundary frame elements were designed in accordance with the requirements of the AISC Manual of Steel Construction (AISC 2005b) and the procedure outlined in the AISC Design Guide (Sabelli and Bruneau 2006) with the yield force of the infill plate, $F_y t_w$, distributed along the length of the VBE and horizontal boundary frame elements (HBE) at the angle of web yielding, α along with other relevant load considerations (e.g., gravity load).

Table 1. Summary of Prototype SPSW

Story	Required t_w (mm)	Specified t_w (mm)
1	4.3	4.8
2	3.8	4.8
3	3.0	4.8
4	1.8	4.8

SPSW Specimens

Two single-story SPSW specimens were proportioned based on the first story of the prototype SPSW and fabricated for the experimental portion of the investigation. The length scale factor of 0.4 was dictated by the desire to use a 1.68 m high existing reaction frame located at the test site and budget considerations. As a result, an ASTM A1011 Gauge 14 sheet with nominal thickness of 1.9 mm (0.075 in) was used for the infill plate of the SPSW specimens.

The HBE and VBE sections of the SPSW specimens were chosen to match, as closely as possible, the scaled properties of the prototype SPSW boundary frame elements as well as meeting the requirements of the Seismic Provisions (AISC 2005a) and the Manual of Steel Construction (AISC 2005b). Fig. 1 shows the two SPSW specimens side by side (as installed against the reaction frame at the test site). Each specimen consists of S200 $\times$24 (S8$\times$23) top and bottom HBE with RBS (reduced beam section) connection details, two W360$\times$79 (W14$\times$53) VBEs, four L76$\times$51$\times$4.8 (L3$\times$2$\times$3/16) fishplates, and a 1,372 mm $\times$1,270 mm infill plate with measured thickness of 2 mm (0.082 in.). The SPSW specimens were cast into a 610-mm-wide $\times$457-mm-deep$\times$4,876-mm-long reinforced concrete foundation beam that was buried in the ground at the test site providing restraint against translation and rotation in the out-of-plane direction. Details of the RBS connection and fishplate are shown in Fig. 2. The infill plate was connected to the L76$\times$51$\times$4.8 fishplate through a fillet weld around the entire perimeter of the infill plate, as typical of seismic detailing. To ensure fusion without "melting away" the edge of the 2-mm plate, the energy of the arc was directed toward the thicker fishplate and the puddle of welding material was manipulated to roll on top of the thinner plate. This procedure was done by an experienced certified welder.

Material testing was performed on the infill plate to determine the mechanical properties of the steel, namely, the yield (F_y) and ultimate (F_u) strengths. Fig. 3 presents the results of uniaxial tension testing performed on two coupons, one cut transverse to the direction of rolling and the other longitudinal to the direction of rolling. From these tests the yield (F_y) and ultimate (F_u) strengths of the infill plate ranged from 328 to 347 MPa and from 395 to 405 MPa, respectively. For the purpose of the analysis of the out-of-plane resistance and dynamic response of the infill plate, the yield and ultimate strengths measured from uniaxial tension testing were increased by 1.2 and 1.05, respectively, to approximately account for the influence of the high rate of loading on the strength of the material (Mays and Smith 1995).

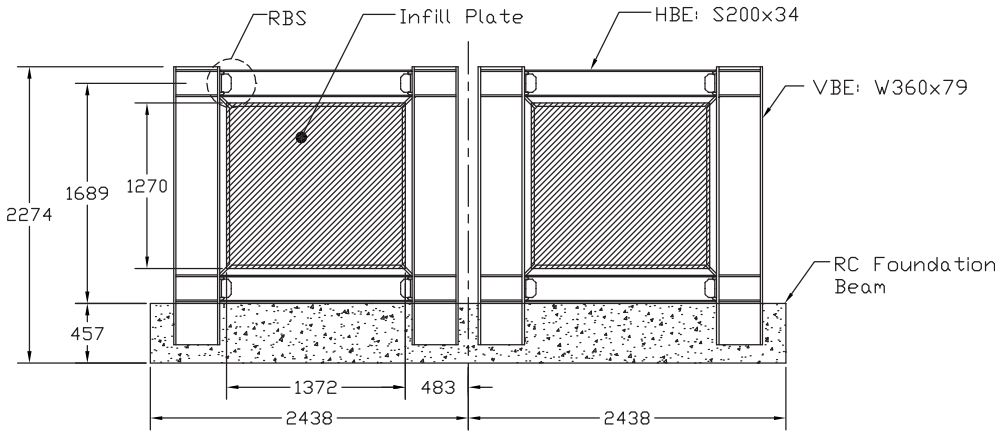

Fig. 1. Illustration of model SPSWs (dimensions in millimeters)

Analysis of SPSW Specimen

Load Resistance

Under lateral seismic or wind in-plane loading, the SPSW infill plate buckles in shear, along the compression diagonal, resulting in the formation of tension field action, along the tension diagonal, that resists the applied lateral load. The loading environment for blast applications differs in that the infill plate is subjected to out-of-plane impulsive pressures that are resisted through membrane or slab action depending on the width-to-thickness ratio of the infill plate. To investigate and model the out-of-plane behavior and strength of SPSW infill plates in planning the experimental program, two traditional analysis techniques were employed for comparison purposes, namely yield line theory and the FE method. Based on the results of these analyses, an approximate plastic analysis procedure was proposed to estimate the out-of-plane resistance of SPSW infill plates.

The resistance of SPSW specimen infill plate was first estimated using yield line theory and the yield line pattern shown in Fig. 4(a), with edges of the plate assumed to be fixed (shown by hatch marks). Per well established principles of yield line analysis (Ingerslev 1923; Park and Gamble 2000), out-of-plane strength is obtained by equating the internal work to the external work assuming a uniform pressure, w. The plastic moment capacity of the plate per unit length is

$$m = \frac{F_y t_w^2}{4} \tag{2}$$

The distance x where the positive moment yield lines intersect each other, corresponding to the minimum energy, can be obtained by equating the internal work to the external work, setting the derivative of w with respect to x, dw/dx, equal to zero and solving for x

$$x = \frac{h}{4L}(-2h + 2\sqrt{h^2 + 3L^2}) \tag{3}$$

The resulting uniform pressure at formation of the yield line mechanism is

$$w = \frac{F_y t_w^2}{xh}\left\{\frac{h^2 + 2Lx}{\frac{hx}{3} + h(L+x)\left[1 - \frac{1}{6}\left(\frac{3L-2x}{L-x}\right)\right]}\right\} \tag{4}$$

For the SPSW infill plate specimen with thickness, t_w, equal to 2 mm and an assumed dynamic yield strength, F_y, equal to 414 MPa, the out-of-plane resistance, w, is estimated to be 0.012 MPa according to yield line theory.

The strength of the SPSW specimen infill plate was further investigated using the general purpose FEA software ABAQUS/Standard [Hibbitt, Karlsson, and Sorenson, Inc. (HKS) 2002a]. The SPSW specimen infill plate was modeled using, approximately, 4,000 three-dimensional eight-node continuum elements (C3D8). The edges of the plate were fixed against translation and rotation. Both geometric and material nonlinearities were considered. The steel material was modeled using a rate-independent plasticity model with a Von Mises yield criteria. The yield, F_y, and ultimate, F_u, strength were both assigned a value of 414 MPa to approximate the dynamic strength of the steel infill material and conservatively assume bilinear elastic perfectly plastic material properties. A static analysis was performed using ABAQUS/Standard where the uniform out-of-plane pressure on the infill

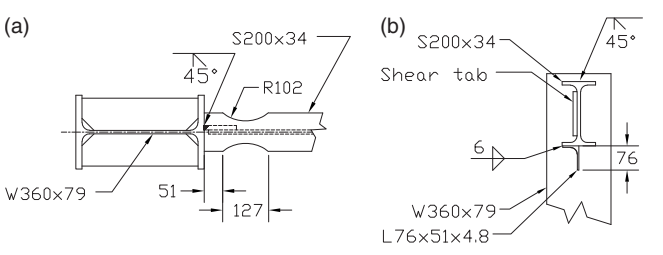

Fig. 2. Model details: (a) RBS Connection; (b) Fishplate (dimensions in millimeters)

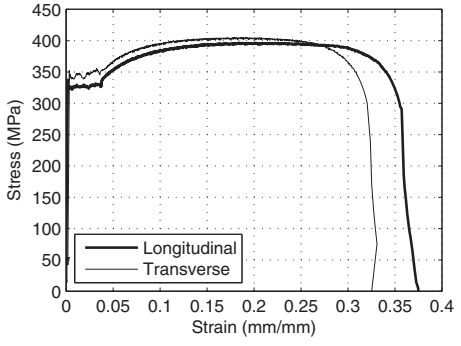

Fig. 3. Results of uniaxial tension test performed on infill plate

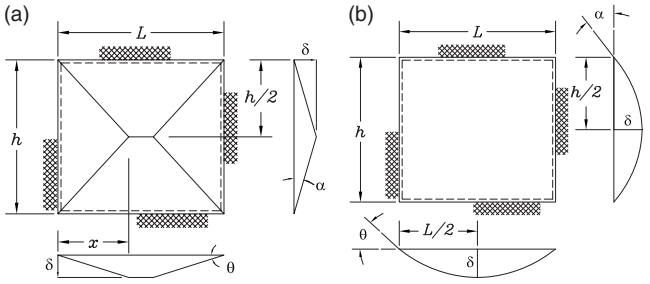

Fig. 4. Plate mechanisms: (a) small deformation; (b) large deformation

plate, w, was incrementally increased and the center displacement of the plate, δ, monitored, reaching a value of 1.32 MPa at 200 mm [Fig. 5(a)]. This is two orders of magnitude more than predicted by the yield line analysis, highlighting the benefits of considering geometric nonlinearities to estimate the out-of-plane resistance of SPSW infill plates. Fig. 5(b) shows corresponding inelastic uniaxial strain at the center of the plate in the vertical direction (direction of largest strain), reaching approximately 0.07 (or 7%) at δ equal to 200 mm. These strain results were used to design the weight and stand-off distance of the explosive charges for the experimental program.

Seeking a simple method to estimate the out-of-plane strength of SPSW infill plates under large deformations without resorting to FEA, an approximate plastic analysis procedure was developed and proposed, in which the deformed shape of the infill plate is approximated using two parabolas. Fig. 4(b) presents an illustration of the assumed deformed shape of the infill plate. Similarly to the yield line mechanism, the center of the plate is assumed to displace a distance δ that also represents the height of the parabola in both the L and h directions. The out-of-plane deformation, $z(x)$, along the L length is defined by the following parabolic equation:

$$z(x) = \frac{4\delta}{L^2}x^2 \tag{5}$$

where x=distance along the L length of the plate. A similar expression can be derived to describe the deformed shape along the h length of the plate. The slope of the parabola at any point, x, is obtained by differentiating Eq. (5) with respect to x

$$\frac{dz(x)}{dx} = \frac{8\delta}{L^2}x \tag{6}$$

The angle or rotation of the parabola at the edge is obtained by taking the arctangent of Eq. (6) and evaluating the expression for $x=L/2$ giving

$$\theta = \tan^{-1}\left[\frac{dz(x=L/2)}{dx}\right] = \tan^{-1}\left(\frac{4\delta}{L}\right) \tag{7}$$

Similarly, the angle of the parabola at the edge, α, in the h direction can be derived and is

$$\alpha = \tan^{-1}\left(\frac{4\delta}{h}\right) \tag{8}$$

Assuming the entire plate to be yielding, the resistance of the plate, w, can be estimated as the out-of-plane component of the yield force acting at angles α and θ as follows:

$$w = \frac{F_y t_w}{Lh}(2L\sin\alpha + 2h\sin\theta) \tag{9}$$

where F_y=yield strength of the plate and t_w=thickness of the infill plate. It is important to note that the above procedure assumes α and θ are constant along the entire length L and h, respectively, when in actuality α and θ are maximum at the center of the plate and decrease toward the edges.

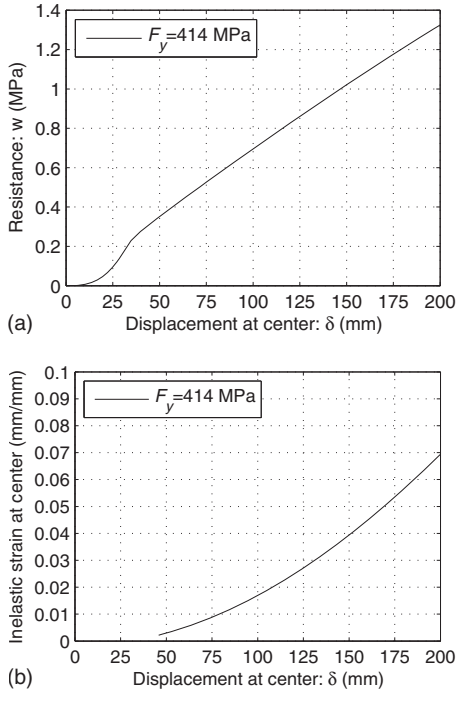

Fig. 5. Sample results of FE analysis: (a) resistance; (b) inelastic strain

Fig. 6 presents a comparison of the estimated out-of-plane resistance using the approximate plastic analysis procedure (shown by a dashed-dot line), FE methods (solid line) and yield line theory (dashed line) for the plausible range of infill plate thicknesses (t_w) for the scaled model. Fig. 6(a) presents a comparison of resistance for the tested infill plate thickness of 2 mm (5 mm at prototype scale) representing the lower bound on plausible infill plate thicknesses for SPSWs. Fig. 6(b and c) present a comparison of resistance for intermediate (3.2 mm) and upper bound (5 mm) infill plate thickness, respectively. The 5 mm infill plate thickness [Fig. 6(c)] represents at prototype scale a 12.5 mm thick infill plate that is considered an upper bound for SPSWs (Sabelli and Bruneau 2006). From the comparisons presented in Fig. 6, the approximate plastic analysis procedure provides a reasonable, albeit slightly unconservative, estimate of the out-of-plane resistance for the plausible range of infill plate thicknesses by comparison to the FE prediction. The overestimation of the approximate plastic analysis procedure can be attributed to the assumption that α and θ are constant along the entire length of the edges. Fig. 6 also shows that yield line theory significantly underestimates the resistance for the range of plausible infill plate thicknesses by comparison to the FE, and is not a recommended procedure to estimate the out-of-plate strength of SPSW infills. Note that a more general investigation of the out-of-plane resistance of plates having a wide range of width-to-thickness ratios, to identify when yield-line theory would start to provide appro-

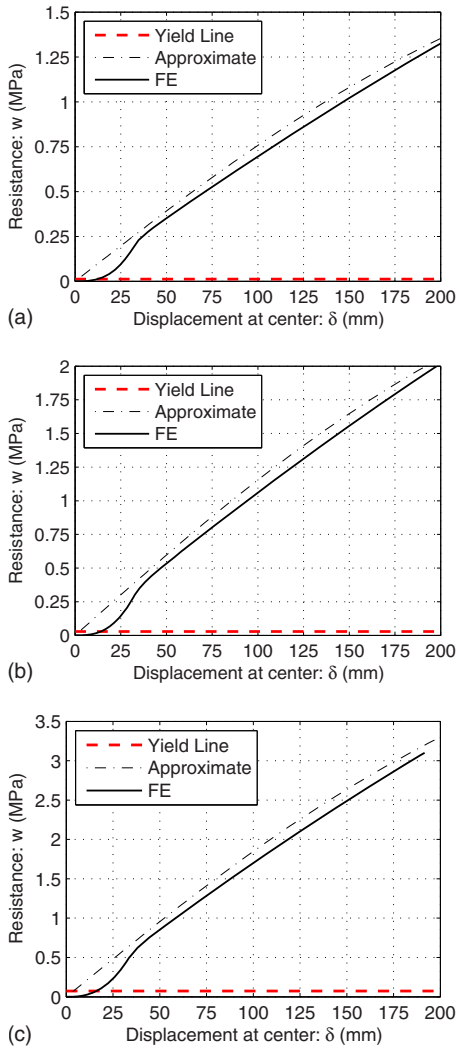

Fig. 6. Comparison of predicted infill plate out-of-plane resistances with plate thickness of: (a) 2 mm; (b) 3.2 mm; and (c) 5 mm

priate results or to quantify a "transition" zone of when it would provide results similar to the approach proposed here, could possibly be valuable, but it is well beyond the scope of the research presented here as it would be applicable only to steel plate walls having exceptionally large infill plate thicknesses as to preclude them from seismic applications.

The approximate plastic analysis procedure also offers the benefit of estimating the average inelastic strain in the plate for a given δ. The length of a parabola, S, along the h length of the plate can be calculated using Eq. (10)

$$S = \frac{1}{2}\sqrt{h^2 + 16\delta^2} + \frac{h^2}{8\delta}\ln\left(\frac{4\delta + \sqrt{h^2 + 16\delta^2}}{h}\right) \tag{10}$$

The average inelastic strain, ε_{in}, can then be estimated according to

$$\varepsilon_{in} = \frac{S - h}{h} - \varepsilon_y \tag{11}$$

where h=dimension of the plate in the direction of consideration and ε_y=yield strain approximately equal to 0.002. For δ equal to 200 mm and h equal to 1,270 mm the inelastic strain, ε_{in}, estimated according to Eqs. (10) and (11) is 0.063 or 6.3%, which compares reasonably well with the inelastic strain at the center of

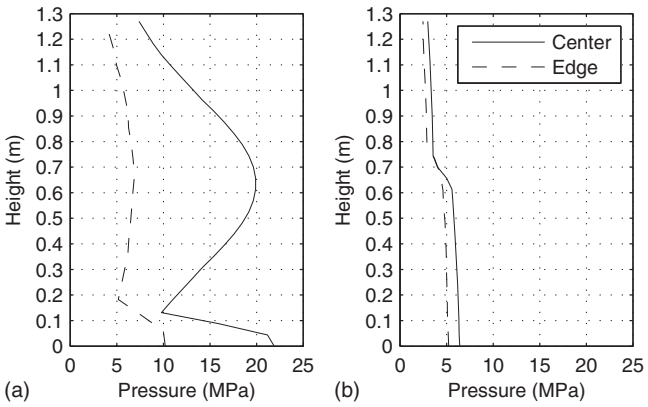

Fig. 7. Variation in peak pressure along height of infill plate: (a) Package; (b) Small Vehicle

the plate of, approximately, 7% predicted by the FE method [see Fig. 5(b)]. Therefore, Eqs. (10) and (11) can be used to relate a limiting value of strain to a displacement at the center for the design of a SPSW infill plate subjected to out-of-plane loading.

Dynamic Response

The characteristics of the dynamic response will depend on both the duration of loading (t_d) and the first mode natural period of the infill plate (T_n) that will vary depending on the specifics of the SPSW and the explosive threat. For the 0.4 scale SPSW model with a first mode natural frequency (f_n) of 10.5 Hz, as determined from plate theory and verified by FEA, the ratio of the loading duration to the first mode period (t_d/T_n) is close to or less than 0.046 (Smith and Hetherington 1994) indicating the loading is predominately impulsive for both explosive charge scenarios considered in this study.

To estimate the demands imposed on the infill plate from an explosive charge of specific weight and stand-off distance, dynamic response-history analysis of the infill plate was conducted using the FE analysis software ABAQUS/Explicit (HKS 2002b). A mesh of 3,000 reduced integration shell elements (S4R) was used together with the same material properties and boundary conditions described previously. The blast loading was simulated using pressure-time histories generated with BEL (Bridge Explosive Loading) software [Bridge Explosive Loading (BEL); version 1.1.0.3 2004] that accounts for reflection surfaces and the angle of incidence in the reflected overpressure calculation. Fig. 7 presents variation in the peak pressure along the height of the infill plate for the *Package* [Fig. 7(a)] and *Small Vehicle* [Fig. 7(b)] explosive charge scenarios. In Fig. 7, the peak pressure distribution is plotted for the center of the infill plate (solid line) and the edge of the infill plate (dashed line) to provide an idea of the distribution of peak pressure in the horizontal direction. From Fig. 7(a) (Package) the peak pressure at the center of the infill plate varies from approximately 22 MPa at the base to 7.5 MPa at the top. The 22 MPa peak pressure at the base is a result of the reflection of the blast wave front off the ground surface in front of the infill plate. From Fig. 7(b) (Small Vehicle) the peak pressure distribution is closer to uniform than the Package scenario as would be expected from the larger stand-off distance. For the Small Vehicle scenario the peak pressure at the center varies from approximately 6.5 MPa at the base to 3 MPa at the top indicating some elevation in the peak pressure due to reflection of the blast wave front off the ground surface but not

(a) (b)

Fig. 8. Photographs of the SPSW specimens installed at test site: (a) elevation; (b) side view showing reaction frame

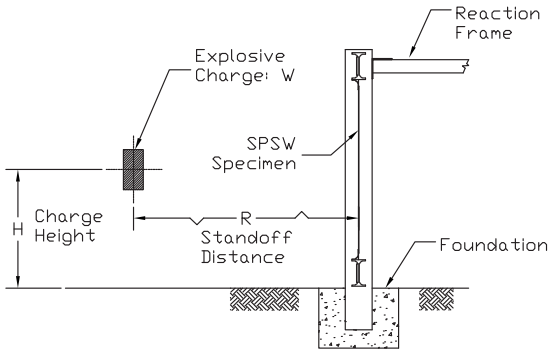

Fig. 9. Experimental specimen and explosive charge placement scenario

as dramatic as with the Package scenario. To account for the variable arrival time of the wave front, the plate was divided into a 10×10 grid and individual pressure-time histories generated with BEL were applied to each region. Although not presented in this paper, the results of preliminary FE analyses performed on a separate but similar model using both a 10×10 and finer discretization of the pressure distribution did not result in substantially different predictions of the peak values (i.e., peak inelastic strain, out-of-plane deformation). Based on the results of these preliminary analyses, it was judged that the 10×10 discretization was sufficient for the nonlinear dynamic FE analyses. Predicted inelastic elongation demands are presented in the following section where they are compared with results from the experimental program.

Experimental Testing

Program and Setup

Fig. 8(a) shows a front elevation the two SPSW specimens installed at the test site. A side view of the SPSW specimens installed against the reaction frame is presented in Fig. 8(b). The foundation beam was buried in the soil to provide lateral support at the base and the top of the specimens were prevented from translation by contact with the steel reaction frame at the approximate midheight of the top HBE.

The experimental program consisted of two tests, the first representing a hand placed explosive charge in close proximity to the target referred to herein as Package and the second representing a vehicle bomb parked at a curbside standoff distance from the target referred to herein as Small Vehicle. Table 2 presents summary information for the tests including: test number, specimen, charge weight, W, standoff distance, R and charge height, H. For security purposes, exact values of the charge weights, W, and standoff distances, R, have been omitted and are instead presented as multiples of generic variables for the smallest charge and distance. Additionally values of the scaled distance, Z, that is calculated according to

$$Z = \frac{R}{W^{1/3}} \tag{12}$$

are not reported in this paper for security purposes. Fig. 9 shows the experimental specimen and the placement of the blast charge.

Observations and Results

The Package explosive test was conducted first on SPSW 1. It was decided to detonate the smaller charge first in close proximity to SPSW 1 in order to minimize loading SPSW 2 given the close proximity of the two SPSW specimens. Fig. 10 shows the backside of SPSW 1 before [Fig. 10(a)] and after [Fig. 10(b)] Test 1. Both photographs also show the 100 mm $\times$ 100 mm grid that was painted on both sides of the infill plate to provide a visual reference for the deformed shape and to aid in the post test measurements. Fig. 10(b) shows that the infill plate sustained significant inelastic deformations yet remained intact and attached to the boundary frame. The profile of the infill plate as it reached peak deformation could not be determined because real-time data was not collected and the final profile "state" of the infill plate was significantly influenced by the negative pressure phase of the explosive loading. However from post test inspection significant out-of-plane deformations were observed over a large portion of the plate not just in the center although the largest deformation was observed at the center qualitatively agreeing with parabolic assumption. For these reasons the authors choose to use the residual in-plane inelastic deformation because this metric is the best indicator of the peak deformation demand and unaffected by the negative pressure phase of the loading on the infill plate.

Significant deformations were observed in the bottom HBE that can be seen in Fig. 10(b). The deformations in the bottom HBE were greater than the top HBE and the difference can be attributed to the increased demand on the bottom HBE due to the reflection of the blast wave front off the soil and concrete surfaces in front of the specimen as suggested in Fig. 7(a). Fig. 11 shows a crack in the complete joint penetration groove welds connecting

Table 2. Blast Test Details

Test number	Description	Specimen	Charge weight W	Standoff distance R	Charge height H (m)
1	Package	SPSW 1	W	R	0.9
2	Small Vehicle	SPSW 2	$3W$	$2.4R$	0.9

(a) (b)

Fig. 10. Photographs of the backside of SPSW 1: (a) before; (b) after

the top flange of the bottom HBE to the column flange; such cracks were observed at both ends of the bottom HBE element.

Fig. 12 shows the front side of SPSW 2 before [Fig. 12(a)] and after [Fig. 12(b)] the Small Vehicle test. Failure occurred at the weld connecting the infill plate to the fishplate around three quarters of the perimeter of the plate. Again, significant inelastic deformation was observed in the bottom HBE element and is apparent from Fig. 13(a). Similar to SPSW 1, weld fractures were observed in the complete joint penetration groove weld connecting the top flange of the HBE element to the flange of the column (VBE). The weld fractures in the SPSW 2 specimen were significantly larger and more pronounced that were observed in SPSW 1 with clear separation (opening) of the crack.

The primary data quantities obtained from the tests were the residual out-of-plane deformation of the center of the plate and the inelastic uniaxial elongation of the vertical and horizontal centerlines of the infill plates. Both quantities were measured after the test using flexible and semirigid measuring tape. From Test 1 (Package), the maximum residual out-of-plane deformation occurred at the center of the plate and was measured to be 133 mm. The length of the plate along the horizontal and vertical centerlines were measured and used to calculate the average inelastic uniaxial strain according to

Fig. 11. Photograph of SPSW 1 bottom beam flange fracture

(a) (b)

Fig. 12. Photographs of the front side of SPSW 2: (a) before; (b) after

$$\varepsilon_{\text{in}} = \frac{L_f - L_i}{L_i} \tag{13}$$

where L_f and L_i=final and initial length of the plate along either the horizontal or vertical centerline. Using Eq. (13) the average inelastic uniaxial strain at the center of the plate in the horizontal and vertical directions were calculated to be 2 and 1.2%, respectively. From Test 2 (Small Vehicle), the measured length of the plate along the horizontal centerline was determined to be approximately equal to the original length, suggesting that the welds failed prior to the development of significant plate yielding. The length of the vertical centerline of the infill plate of SPSW 2 could not be measured.

Table 3 presents a comparison of the experimental and FE results. The FE analysis results for Test 1 are shown to over predict the average inelastic uniaxial strain along both the horizontal and vertical centerlines. For the horizontal and vertical centerlines, respectively, the FE analysis predicted 2.9 and 3.1%, in comparison to the obtained experimental values of 2 and 1.2%. From geometry the strain in the vertical direction would be expected to be larger than the strain in the horizontal direction for a given center out-of-plane displacement because the height of the infill plate is less than its width. However, the experimental results show the opposite, with the strain in the horizontal direction (2%) larger than in the vertical direction (1.2%). A possible explanation for this discrepancy might be related to the flexibility of the boundary frame in that the HBEs (S8×23), being considerably less stiff in bending and torsion than the VBEs (W360×79), could have been less effective in restraining the

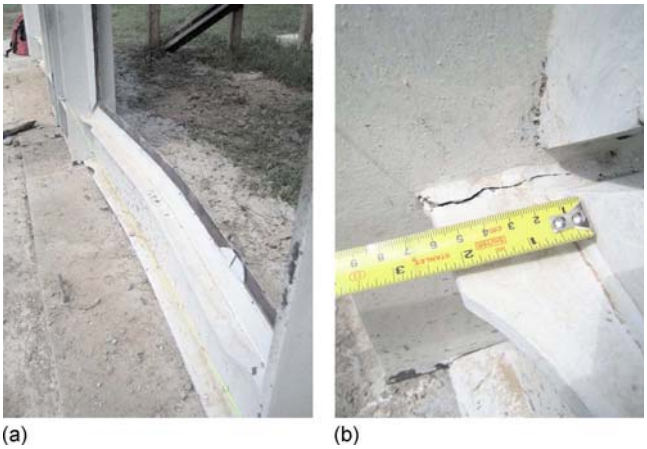

(a) (b)

Fig. 13. Photograph of SPSW 2 following Test 2: (a) bottom beam; (b) weld fracture beam-column connection

Table 3. Comparison of Results

Test number	Specimen	Average inelastic strain (%)			
		Experimental		FE	
		Horizontal	Vertical	Horizontal	Vertical
1	SPSW 1	2	1.2	2.9	3.1
2	SPSW 2	0	N/A	3.2	3.8

Note: N/A=not available.

plate in the vertical direction. No comparison of results is provided for Test 2 due to the failure of the fillet weld connecting the infill plate to the fishplate prior to the development of significant inelastic deformations.

Investigation of the Failure Surface

To investigate the failure of the infill plate to fishplate connection, a section of the fishplate on the bottom HBE of SPSW 2 was removed to facilitate viewing the failure surface using a scanning electron microscope (SEM). Fig. 14(a) shows the front elevation of SPSW 2 following Test 2. The section of fishplate removed from the right side of the bottom HBE is shown in Fig. 14(b). It can be seen in Fig. 14(b) that small portions of the infill plate remained connected to the fishplate with the failure surface occurring in the infill plate material, however, the failure surface occurred in the fillet weld along the majority of the length of the infill plate. Two sections were investigated with the SEM [Fig. 14(b)]: Section S3 where failure occurred in the fillet weld, and; Section S4 where failure occurred in the infill plate material. Although not presented here, analysis of the failure surface at section S4 suggested failure due to tensile overloading with clear indications of necking at 100× magnification and a cup-cone failure surface with some indications of directionality at 1,000× magnification. Fig. 14(c) presents a 45× magnification view looking at the S3 failure surface in the direction indicated by the arrow shown in Fig. 14(b). Fig. 14(c) shows a 45° shear surface on the left side and a 0° surface on the right that shows voids indicating incomplete weld fusion. Fig. 14(d) presents a 1,000× magnification of the 0° surface on the right side of Fig. 14(c), showing evidence of ductility, apparent from the cup-cone failure surface, and smooth surfaces that represent solidified weld metal and incomplete weld fusion.

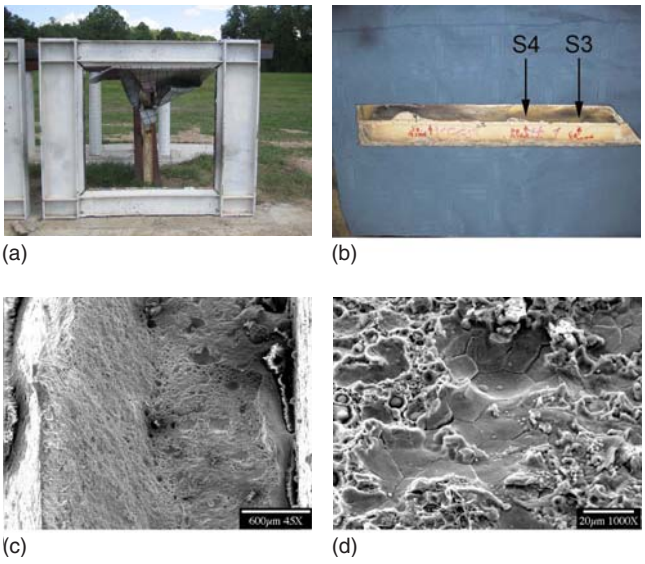

(a) (b) (c) (d)

Fig. 14. Photograph of SPSW 2 following Test 2: (a) front elevation; (b) removed fishplate section; (c) 45× view of Section S3; and (d) 1,000× view of 0 degree base at Section S3

In the opinion of one metallurgical engineer (R. C. Wetherhold, Dept. of Mechanical and Aerospace Engineering, University at Buffalo, personal communication), while the weld showed areas of high quality, the evidence of incomplete fusion along the length of the weld suggests that performance could have been better. However, in reviewing this data, an experienced welding design consultant (Dr. Duane Miller, The Lincoln Electric Company, personal communication) commented that, "while the evidence of incomplete fusion could be problematic, it cannot be determined whether this incomplete fusion could have by itself triggered the failure. The crack initiation point for the entire plate is unknown (and would be hard to identify for such thin material). Once failure has initiated, the running crack is likely to propagate through points of discontinuities and incomplete fusion, yet these local discontinuities in the weld could have been able to resist cracking had the crack not initiated elsewhere." Note that fillet welds are routinely only visually inspected—when inspection of fillet welds is called for, magnetic particle inspection is a typical methodology for steel weldments. For the 2-mm thick plate used for the specimens, both Ultrasonic Testing inspection and Magnetic Particle inspection cannot be practically done—these methods would not have likely been able to detect the defects shown in Fig. 14 using the procedures conducted on a commercial basis. The best approach when welding such thin material is to control the quality of the welding procedure (Dr. Duane Miller).

As such, it is not possible to establish with certainty whether the weld quality had an impact on the observed failure. However, the experimental results underscore the need to develop alternative weld designs able to develop full capacity of the connected SPSW infill plate thin plate for combined seismic and blast applications.

Summary and Conclusions

Analytical and experimental investigations of the blast resistance of a SPSW designed for seismic loading were presented. A comparison of the results of the nonlinear FE analysis with the resistance predicted by yield line theory showed that yield line theory significantly underestimated the out-of-plane resistance and that yield line theory is not an appropriate analysis technique for plates with similar aspect ratios to the SPSW specimen infill plate investigated in this study. An approximate plastic analysis procedure whereby the deformed shape of the infill plate is approximated by two parabolas was proposed and shown to agree

well with the results of FE analysis in terms of the predicted out-of-plane resistance and the inelastic uniaxial strain along the centerlines.

The experimental investigation showed that a SPSW designed for seismic loading has a limited capacity to resist out-of-plane blast loading as was observed from the Package sized explosive charge. Results from the Package sized experimental test indicates potentially promising performance of SPSW infills under localized and nonuniform loading as suggested by the peak pressure distribution for the Package scenario. Although the SPSW performed well under the Package scenario presented in this paper, more research is needed to fully understand the behavior of SPSW infill plates under varying conditions of highly localized and highly nonuniform blast loading. Results of the Small Vehicle test showed the capacity of the SPSW to resist out-of-plane blast loading is limited not by the ductility of the infill plate but rather by the connection of the infill plate to the boundary frame and that defects in the weld could serve as points of failure initiation that might propagate around the perimeter of the infill plate causing partial or complete failure. Special attention should be given to the infill plate to boundary frame connection for blast applications and future research should be conducted to investigate a connection detail that would be appropriate for multihazard applications.

Although not supported by experimental data, due to a lack of real-time data acquisition, the reaction forces of the infill plate generated from an explosive charge causing out-of-plane deformations should be limited to the dynamic yield strength of the infill plate and the angle of rotation of the infill plate at the support. The approximate plastic analysis procedure presented in this paper provides a methodology of determining the reaction forces that would be generated and an estimation of the peak angle at which they occur. The yield strength of the plate and the angle of rotation can then be used to design the boundary frame to withstand the reaction forces generated during an explosive event highlighting one of the potential benefits that SPSWs as blast resistant walls offer over alternative reinforced curtain wall systems.

Acknowledgments

This work was supported in part by the Earthquake Engineering Research Centers Program of the National Science Foundation under Grant No. ECC-9701471 to the Multidisciplinary Center for Earthquake Engineering Research. However, any opinions, findings, conclusions, and recommendations presented in this paper are those of the writers and do not necessarily reflect the views of the sponsors. Special thanks are given to James C. Ray at the Eng. Research Dev. Center of the USACE for his help and assistance in the logistics of the experiments.

References

AISC. (2005a). *Seismic provisions for structural steel buildings*, Chicago.

AISC. (2005b). *Manual of steel construction*, 13th Ed., Chicago.

ASCE. (2005). "Minimum design loads for buildings and other structures." *ASCE 7–05*, Reston, Va.

Berman, J. W., and Bruneau, M. (2003). "Experimental investigation of light-gauge steel plate shear walls for the seismic retrofit of buildings." *Technical Rep. MCEER-03–0001*, Multidisciplinary Center for Earthquake Engineering Research, Buffalo, N.Y.

Bridge Explosive Loading (BEL); version 1.1.0.3. (2004). U.S. Army Corps of Engineers, Engineering Research and Development Center, Vicksburg, Miss.

Driver, R. G., and Grondin, G. Y. (2001). "Steel plate shear walls: Now performing on the main stage." *Modern steel construction*, AISC, Chicago.

Driver, R. G., Kulak, G. L., Kennedy, D. J. L., and Elwi, A. E. (1997). "Seismic behaviour of steel plate shear walls." *Structural Engineering Rep. No. 215*, Dept. of Civil Engineering, Univ. of Alberta, Edmonton, Alberta, Canada.

FEMA. (2003). "NEHRP recommended provisions for seismic regulations for new buildings and other structures. 1: Provisions and 2: Commentary." *FEMA 450*, Washington, D.C.

Fujikura, S., Bruneau, M., and Lopez-Garcia, D. (2008). "Experimental investigation of multihazard resistant bridge piers having concrete-filled steel tube under blast loading." *J. Bridge Eng.*, 13(6), 586–594.

Hibbitt, Karlsson, and Sorenson, Inc. (HKS). (2002a). "ABAQUS/Standard users' manual." Version 6.3, Hibbitt, Karlsson, and Sorenson, Inc., Pawtucket, R.I.

Hibbitt, Karlsson, and Sorenson, Inc. (HKS). (2002b). "ABAQUS/Explicit users' manual." Version 6.3, Hibbitt, Karlsson, and Sorenson, Inc., Pawtucket, R.I.

Ingerslev, A. (1923). "The strength of rectangular slabs." *Struct. Eng*, 1(1), 3–14.

Mays, G. C., and Smith, P. D. (1995). *Blast effects on buildings—Design of buildings to optimize resistance to blast loading*, Telford, London.

Norville, H. S., and Conrath, E. J. (2006). "Blast-resistant glazing design." *J. Archit. Eng.*, 12(3), 129–136.

Park, R., and Gamble, W. L. (2000). *Reinforced concrete slabs*, 2nd Ed., Wiley, New York.

Rogers, R. L. (2002). "Building his profession." *Innovation: J. Assoc. Professional Engineers and Geoscientists of British Columbia*, 6(2), 14–16.

Romero, E. M. (2003). "Construcción compuesta en edificios altos." *Proc., VII Simposio Internacional de Estructuras de Acero*, Veracruz, Mexico.

Sabelli, R., and Bruneau, M. (2006). "Steel plate shear walls." *Steel design guide*, American Institute of Steel Construction, Chicago.

Schumacher, A., Grondin, G. Y., and Kulak, G. L. (1999). "Connection of infill panels in steel plate shear walls." *Can. J. Civ. Eng.*, 26(5), 549–563.

Seilie, I. F., and Hooper, J. (2005). "Steel plate shear walls: Practical design and construction." *Modern Steel Constr.*, 45(4), 37–43.

Simmons, L., Woodson, S., and Sinno, R. R. (2008). "Reinforcing building facades with geotextile fabrics." *J. Archit. Eng.*, 14(2), 53–60.

Smith, P. D., and Hetherington, J. D. (1994). *Blast and ballistic loading of structures*, Butterworth-Heinemann, Oxford, U.K.

Starr, C. M., and Krauthammer, T. (2005). "Cladding-structure interaction under impact loads." *J. Struct. Eng.*, 131(8), 1178–1185.

Timler, P. A., and Kulak, G. L. (1983). "Experimental study of steel plate shear walls." *Structural Engineering Report No. 114*, Dept. of Civil Engineering, Univ. of Alberta, Edmonton, Alberta, Canada.

Wanitkorkul, A., and Filiatrault, A. (2008). "Influence of passive supplemental damping systems on structural and nonstructural seismic fragilities of a steel building." *Eng. Struct.*, 30(3), 675–682.

Williams, D., Holland, C., Williamson, E., Bayrak, O., Marchand, K., and Ray, J. (2008). "Blast-resistant highway bridges: Design and detailing guidelines." *Proc., 10th Int. Conf. on Structures under Shock and Impact (SUSI)*, Algarve, Portugal.

Woodson, S. C., and Baylot, J. T. (1999). "Structural collapse: Quarter-scale model experiments." *Technical Rep. No. SL-99–8*, U.S. Army Engineer Research and Development Center, Vicksburg, Miss.

Yang, T. Y., and Whittaker, A. (2002). "MCEER demonstration hospitals—Mathematical models and preliminary analysis results." *Technical Rep.*, Multidisciplinary Center for Earthquake Engineering Research, Univ. at Buffalo, Buffalo, N.Y.